Title

Transportation Impacts of Berkeley Hills Tunnel Disruption by Earthquakes

Authors

Han, Tianyu

Zhao, Bingyu, PhD

Tang, Yili (Kelly), PhD

et al.

Publication Date

2026-08-01

DOI

10.7922/G2J964SM

RESEARCH REPORT

Institute of Transportation Studies | UNIVERSITY OF CALIFORNIA

Transportation Impacts of Berkeley Hills Tunnel Disruption by Earthquakes

Tianyu Han, Ph.D. Candidate [1], Bingyu Zhao, Ph.D.[2], Yili (Kelly) Tang, Ph.D.[3], Ph.D., Louise Comfort, Ph.D.[4], and Kenichi Soga, Ph.D.[1]

[1]University of California, Berkeley
[2]Technische Universität Wien
[3]University of Western Ontario
[4]University of Pittsburgh

August 2026

UC Berkeley
Institute of
Transportation Studies

Report No.: UC-ITS-2024-14 | DOI: 10.7922/G2J964SM

Technical Report Documentation Page

1. Report No.	2. Government Accession No.	3. Recipient's Catalog No.
UC-ITS-2024-14	N/A	N/A

4. Title and Subtitle	**5. Report Date**
Transportation Impacts of Berkeley Hills Tunnel Disruption by Earthquakes	August 2026
	6. Performing Organization Code ITS Berkeley
7. Author(s) Tianyu Han, https://orcid.org/0009-0007-2307-6322; Bingyu Zhao, Ph.D., https://orcid.org/0000-0002-2369-7731; Yili (Kelly) Tang, Ph.D., https://orcid.org/0000-0002-5343-6823; Louise Comfort, Ph.D., https://orcid.org/0000-0003-4411-1354; Kenichi Soga, Ph.D., https://orcid.org/0000-0001-5418-7892	**8. Performing Organization Report No.** N/A
9. Performing Organization Name and Address Institute of Transportation Studies, Berkeley 109 McLaughlin Hall, MC1720 Berkeley, CA 94720-1720	**10. Work Unit No.** N/A
	11. Contract or Grant No. UC-ITS-2024-14
12. Sponsoring Agency Name and Address The University of California Institute of Transportation Studies www.ucits.org	**13. Type of Report and Period Covered** Final Report (December 2023 – December 2025)
	14. Sponsoring Agency Code UC ITS

15. Supplementary Notes

DOI: 10.7922/G2J964SM

16. Abstract

In the San Francisco Bay Area, earthquake damage to a small number of critical transportation facilities can produce regionwide mobility impacts. This report evaluates the Berkeley Hills Tunnel, a key Bay Area Rapid Transit (BART) cross-hills connection, using an integrated model that links tunnel seismic performance to transportation consequences during disruption and recovery. The model couples scenario-based seismic assessment of the tunnel with screening-level fragility for substitute corridors and propagates the resulting time-dependent capacity states through a transportation simulation. At a representative recovery-stage demand of 25 percent of normal, mean cross-hills travel time rises from about 9 minutes in the mildest scenario (327-year return period) to about 41 minutes in the most severe (654-year). In that severe case, a fully subscribed bus bridge can lower the mean cross-hills travel time by up to 30 percent. Uncertainty quantification identifies recovery-stage demand as the dominant source of travel-time variance and shows that unfavorable capacity combinations can nearly double travel time relative to the central estimate. Disruption falls disproportionately on transit-dependent travelers, who either endure longer travel times or pay an extra travel fee. Agencies can use the workflow to assess disruption impacts and identify likely bottlenecks, compare recovery-stage operational strategies, and target equitable service for affected populations.

17. Key Words	**18. Distribution Statement**
Earthquakes, Earthquake engineering, Tunnels, Hills, Rail transit, Highways, Disaster resilience, Service disruption, Computer models	No restrictions.

19. Security Classification (of this report)	20. Security Classification (of this page)	21. No. of Pages	22. Price
Unclassified	Unclassified	51	N/A

Form Dot F 1700.7 (8-72) Reproduction of completed page authorized

About the UC Institute of Transportation Studies

The University of California Institute of Transportation Studies (UC ITS) is a network of faculty, research and administrative staff, and students dedicated to advancing the state of the art in transportation engineering, planning, and policy for the people of California. Established by the Legislature in 1947, ITS has branches at UC Berkeley, UC Davis, UC Irvine, and UCLA.

Acknowledgments

This study was made possible with funding received by the University of California Institute of Transportation Studies from the State of California through the Road Repair and Accountability Act of 2017 (Senate Bill 1). The authors would like to thank the State of California for its support of university-based research, and especially for the funding received for this project. The authors would also like to thank Dr. Esra Zengin, Professor Yousef Bozorgnia, and Professor Jonathan P. Stewart from University of California, Los Angeles for their invaluable collaboration on the structural analysis of the Berkeley Hills Tunnel in this project. The authors also thank Postdoctoral Scholar from California Institute of Technology Jinyan Zhao for his support in the seismic assessment of transportation facilities using SimCenter tools. Finally, the authors would like to thank experts from Bay Area Rapid Transit (BART) and California Department of Transportation (Caltrans) for their valuable insights and contributions.

Disclaimer

Institute of Transportation Studies | UNIVERSITY OF CALIFORNIA

Transportation Impacts of Berkeley Hills Tunnel Disruption by Earthquakes

Tianyu Han, Ph.D. Candidate [1], Bingyu Zhao, Ph.D.[2], Yili (Kelly) Tang, Ph.D.[3], Ph.D., Louise Comfort, Ph.D.[4], and Kenichi Soga, Ph.D.[1]

[1]University of California, Berkeley
[2]Technische Universität Wien
[3]University of Western Ontario
[4]University of Pittsburgh

August 2026

UC Berkeley Institute of Transportation Studies

Report No.: UC-ITS-2024-14 | DOI: 10.7922/G2J964SM

Table of Contents

Table of Contents

List of Tables

List of Figures

Executive Summary

Executive Summary

Earthquakes pose a major threat to the San Francisco Bay Area (the Bay Area) transportation system because damage to a small number of critical corridors can produce large, regionwide mobility impacts. The Berkeley Hills Tunnel is a critical Bay Area Rapid Transit (BART) asset that supports cross-hills connectivity between the inner East Bay and Contra Costa County. Its seismic performance is therefore a key consideration for resilience planning because disruption can reduce cross-hills capacity and shift travel to substitute corridors with limited spare capacity, degrading accessibility and increasing travel times during recovery. Stakeholder interviews conducted in this study also indicated that recovery-stage coordination can be challenging in the Bay Area's multi-agency environment and that formalized recovery planning and cross-agency coordination mechanisms remain limited. This report combines seismic engineering analysis with transportation simulation to translate tunnel performance under seismic loading into transportation-system consequences during the recovery stage. The resulting integrated model supports scenario-based recovery planning by connecting engineering-informed damage and restoration assumptions to mobility outcomes and by helping agencies compare feasible operational strategies and coordination needs across the recovery timeline.

The study integrates three components. The first component is the seismic performance evaluation of the Berkeley Hills Tunnel, carried out by project collaborators at the University of California, Los Angeles (UCLA). This work evaluates tunnel response under fault-displacement scenarios and characterizes damage progression, expected operational constraints, and restoration timelines (Zengin et al., 2025). The resulting engineering assessments are translated into scenario-based rail service states that represent capacity restrictions and recovery durations. The second component is the assessment of alternative cross-hills routes. This analysis estimates the post-earthquake operability of substitute corridors, including State Route 24 (SR 24) through the Caldecott Tunnel and selected local Berkeley Hills roadways, using screening-level fragility relationships and regional ground-failure modeling approaches under the same earthquake scenarios. The third component is the transportation consequence analysis. In this step, the time-dependent capacity states derived from the tunnel and roadway assessments are implemented with a transportation simulation model developed in Phase 1 of this project. A user-equilibrium assignment is included to better represent recovery-stage route choice under congestion and evolving network constraints.

At a representative recovery-stage demand of 25 percent of normal, mean cross-hills travel time rises from about 9 minutes at the mildest scenario (327-year return period) to about 41 minutes under severe disruption (654-year), with intermediate scenarios at about 20 and 23 minutes. A representative case study evaluates bus-bridging mitigation under the most severe scenario, where a fully subscribed bus bridge that carries all displaced rail riders lowers the mean cross-hills car travel time from about 41 to about 29 minutes, roughly a 30 percent reduction, and cuts road loading by about 25 percent. This is an upper-bound benefit that eases roadway strain.

Because post-earthquake operating conditions and travel demand during recovery are both uncertain, the report quantifies how that uncertainty shapes the results, using forward propagation with Latin hypercube sampling. Holding demand at a representative level and varying the cross-hills roadway capacities produces a range of possible travel times rather than a single estimate, and shows that unfavorable capacity combinations can nearly double recovery-stage travel time relative to the central estimate, so planning should account for this downside. A variance-based sensitivity analysis that also treats demand as uncertain identifies recovery-stage demand as the dominant driver of travel-time variability.

Overall, this report demonstrates a transferable workflow that links fault-displacement-based tunnel performance modeling to transportation impacts and recovery-stage planning measures that are interpretable to practitioners. The model is modular. As higher-resolution fragility, functionality, and restoration information becomes available for additional assets, those inputs can replace screening assumptions without changing the overall modeling architecture. The results support resilience planning by identifying which corridors and operational strategies most influence recovery-stage mobility and by providing a structured approach to uncertainty quantification that can guide priorities for data collection and model refinement. The report also examines how disruption distributes inequitably across travelers. Because many do not have access to a personal vehicle and no parallel transit serves the corridor, transit-dependent riders either endure longer travel times on a bus bridge, where one is available, or pay more for a ride-hail trip.

Contents

1 Introduction

1.1 Earthquake Context in California and the San Francisco Bay Area

California experiences frequent earthquakes due to relative motion between the Pacific Plate and the North American Plate. This motion occurs primarily along the San Andreas Fault system and associated faults. Many of the state's major population and employment centers are located near these active fault systems. As a result, transportation infrastructure is routinely exposed to strong ground shaking, permanent ground deformation, and cascading disruption to the mobility of goods, services, and people.

In the Bay Area, the risk of earthquakes is high over planning time horizons. The United States Geological Survey (USGS) estimated a 72 percent probability of at least one magnitude 6.7 or larger earthquake in the Bay Area between 2014 and 2043 (USGS, 2016). **Figure 1** summarizes this regional hazard context. The Bay Area's physical geography and built environment can also amplify the consequences of transportation damage. Water crossings and mountainous terrain limit route redundancy, and dense development concentrates travel demand on a small number of corridors. As a result, disruption to a small set of links can produce regionwide mobility impacts (USGS, 2016).

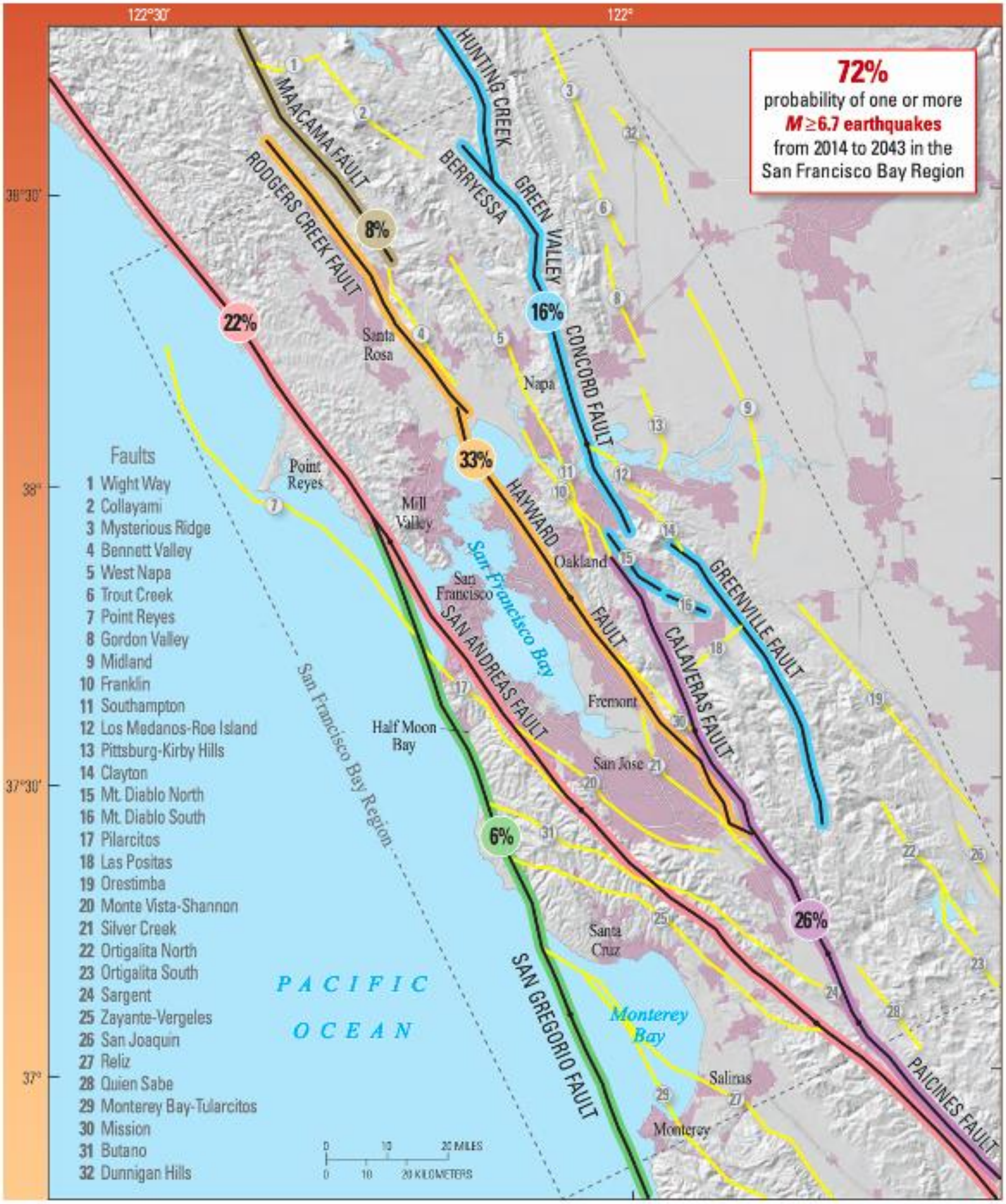

Figure 1. Map of Known Active Faults and Earthquake Probabilities in the Bay Area (USGS, 2016).

1.2 Impacts of Earthquakes on Transportation System Performance

Earthquakes can reduce transportation system performance through multiple pathways. Ground shaking and permanent ground deformation can damage roads, bridges, tunnels, railways, and terminals. Earthquakes can also trigger geotechnical failures such as landslides and liquefaction that block routes or reduce usable capacity. In addition, agencies may impose operational restrictions to support inspections, emergency access, and public safety. Together, these effects can produce abrupt capacity loss, longer travel times, reduced reliability, and reduced accessibility. These impacts are especially consequential because they can constrain emergency response and early recovery activities that depend on timely access and mobility (McCullough, 1994).

Transportation disruption is rarely confined to the damaged facility. Following major events, travelers adapt by shifting routes, travel schedules, destinations, and sometimes modes. These adjustments can generate spillover congestion on parallel facilities and across the broader network (Giuliano & Golob, 1998). As a result, the societal and economic consequences of an earthquake are often realized through network-level performance degradation over the recovery period, rather than through component-level damage alone (Giuliano & Golob, 1998).

1.3 Tunnel Vulnerability and Network Consequences

Tunnels are critical elements of urban transportation systems, particularly where topography or waterways constrain surface alignments. Although underground structures can be less sensitive to short-period shaking than many surface facilities, tunnel performance can still be governed by ground deformation, fault rupture, soil–structure interaction, groundwater effects, and localized lining distress (Hashash et al., 2001; Owen & Scholl, 1981). Documented damage mechanisms include cracking, lining spalling, joint distress, localized buckling, and groundwater inflow, with collapse possible in severe cases (Owen & Scholl, 1981; Wang et al., 2001).

Earthquake engineering research has focused on understanding these mechanisms, documenting tunnel performance in past events, and improving design and retrofit strategies. Historical earthquakes show that tunnel vulnerability increases when strong shaking coincides with fault displacement, ground failure, or complex geological conditions. The 1995 Hyogo-ken Nanbu (Kobe) earthquake caused substantial damage to underground and subway infrastructure and motivated detailed investigation of tunnel damage processes (Asakura & Sato, 1998; Iida et al., 1996; Uenishi & Sakurai, 2000). Subsequent events, including the 1999 Chi-Chi earthquake, the 1999 Düzce earthquake, and the 2008 Wenchuan earthquake, further documented severe tunnel damage under strong shaking and adverse ground conditions (Ulusay et al., 2002; Wang et al., 2001; Yu et al., 2016). This evidence has supported mitigation approaches such as flexible joints, strengthened linings, and ground stabilization to reduce tunnel risk in active fault environments (Anastasopoulos et al., 2008; Russo et al., 2002).

Transportation and resilience research has, in parallel, examined what happens to system performance when a critical transportation facility is disrupted. When a key link is closed or operates at reduced capacity, travelers shift to the remaining corridors, which may already be near capacity, creating spillover congestion, reduced reliability, constrained emergency access, and broader economic disruption (Giuliano & Golob, 1998; McCullough, 1994). These impacts are not determined by physical damage alone. They also depend on how agencies manage operations during response and recovery, including inspection decisions, interim operating policies, and the pace of restoration (Chang & Nojima, 2001). Accessibility-oriented research further emphasizes that the main consequence for many users is reduced access to essential activities, including work, healthcare, schools, and supply chains (Chang, 2003). Network-risk studies likewise show that when redundancy is limited, disruption of a single link can propagate through the system and shape regional impacts and restoration priorities (Basöz et al., 2007; Werner et al., 2006). Recent modeling work also highlights that recovery outcomes depend on the interaction between restoration decisions and traveler responses as conditions evolve over time (Zhao & Zhang, 2020).

Relatively few studies directly link scenario-based tunnel performance under seismic loading to transportation-system consequences over time in a way that supports recovery planning. This gap makes it difficult to translate fragility, damage states, and restoration assumptions into mobility metrics that are meaningful for operations and investment decisions. This study addresses that gap by presenting an integrated model that links scenario-based seismic performance assessment with transportation simulation.

1.4 Purpose of this Report

Many earthquake engineering studies and planning documents describe how a tunnel might be damaged, including expected damage states, fragility, and repair needs, but they often do not quantify what those outcomes mean for travelers or transportation system performance over time. Recovery planning requires both perspectives: how likely different levels of tunnel damage are under plausible earthquake scenarios and how those damage outcomes translate into mobility impacts during disruption and recovery (Chang & Nojima, 2001; Chang, 2003).

Because resources are limited, agencies must prioritize among retrofit investments, redundant capacity options, inspection and operating strategies, and staged restoration actions based on their expected mobility benefits. For resilience planning, the key questions are how damage affects functionality, how quickly service can be restored, and how those recovery trajectories shape travel time, congestion, and access across the network. A clear modeling approach that links tunnel damage to network performance over the recovery period can support stakeholder coordination and decision making.

To address these needs, this report presents an integrated model that links seismic performance assessment outputs to a transportation simulation model. The Berkeley Hills corridor is used as a case study to demonstrate how scenario-based disruption and recovery inputs from the Berkeley Hills Tunnel assessment can be translated into time-dependent capacity constraints and cross-hills mobility impacts. By integrating engineering-informed functional states with transportation simulation, the report provides a basis for comparing scenarios, evaluating operational mitigation strategies, supporting equitable recovery planning and inter-agency coordination, and prioritizing resilience investment for critical transportation facilities.

1.5 Structure of the Report

Following this introduction, Section 2 summarizes stakeholder perspectives on resilience, coordination, and recovery needs, and Section 3 describes the interdisciplinary collaboration and integrated workflow connecting engineering outputs to transportation modeling inputs. Section 4 introduces the seismic performance assessment of the Berkeley Hills Tunnel conducted by collaborators at UCLA, including the fault-displacement scenarios, expected damage and functionality states, and restoration timelines used to define disruption and recovery conditions. Section 5 describes the possible damage, operability, and recovery of alternative cross-hills routes (SR 24 through the Caldecott Tunnel and representative local roads). Section 6 documents the transportation simulation platform, network and demand inputs, and scenario implementation, including the choice of roadway assignment engine, headline per-scenario travel-time impacts, demand-assumption sensitivity, a representative bus-bridging mitigation case, and uncertainty quantification. The report concludes with a discussion (Section 7) of implications for recovery planning and operations, equity in recovery-stage planning, the modeling approach, and broader regional impact assessment.

2 Stakeholder Perspectives on Resilience, Coordination, and Recovery Needs

To better understand current practices and remaining gaps in the Bay Area transportation resilience and recovery planning, this study draws on stakeholder engagement conducted during the University of California Institute of Transportation Studies (UC ITS) RIMI Phase 1 and follow-up discussions conducted for this study. In the Phase 1 project, we conducted semi-structured interviews with practitioners from regional planning organizations, transit agencies, and related partners, including the Alameda County Transportation Commission, the Metropolitan Transportation Commission, and the San Francisco Bay Area Planning and Urban Research Association (Soga et al., 2024). In these interviews, stakeholders described progress in preparedness activities, while recovery planning was generally less developed and less formalized. Stakeholders also highlighted the value of mutual aid and coordination across agencies but noted that coordination can be challenging in a region with many operators (Soga et al., 2024).

In this study, we conducted follow-up interviews with operation planners at BART and senior engineering staff from California Department of Transportation (Caltrans) to better understand cross-hills disruption and recovery issues. Interviewees explained that emergency response plans are generally more developed than recovery-stage plans, and it is difficult to commit to specific resource levels or restoration timelines in advance. When BART service is disrupted, bus bridge service is typically coordinated through rapid, direct communication among agencies. However, implementing bus bridges at scale may be limited by bus and driver availability, dispatch and staging capacity, and the ability to coordinate quickly across organizations. The interviewees suggested that a shared platform for information sharing and coordination could improve efficiency and support faster decision-making during disruptions. Interviewees also noted that ride-hailing partnerships could help support mobility during recovery, but it may not be easily activated under current policies and contracting arrangements. Finally, they emphasized that recovery timelines can be shaped by practical constraints such as site access, inspection requirements, and the availability of specialized equipment, particularly when surrounding infrastructure is also disrupted.

These stakeholder perspectives reinforce the value of a scenario-based analysis approach that supports planning and coordination by enabling stakeholders to compare disruption and recovery conditions, clarify cross-agency dependencies, and identify where operational constraints could limit the effectiveness of planned strategies.

3 Interdisciplinary Collaboration and Integrated Workflow

This study uses an integrated workflow to connect tunnel seismic performance with transportation impacts and recovery planning. **Figure 2** summarizes this process and shows how hazard and soil–structure modeling for the Berkeley Hills Tunnel is translated into disruption and recovery inputs for the transportation simulation.

The workflow is implemented jointly by geotechnical engineering collaborators at UCLA and transportation researchers at UC Berkeley, with input from the agency stakeholders described in Section 2. The engineering component combines probabilistic seismic hazard analysis with detailed numerical modeling of the tunnel and surrounding ground to estimate strain demands, damage progression, and damage states. These damage outcomes are translated into functionality states that reflect operational conditions such as speed restrictions, partial closures, or full closure, together with associated restoration timelines. The transportation component uses these time-dependent functionality states as scenario inputs to modify network capacity and connectivity and to evaluate impacts on travel time and other mobility performance measures. Stakeholder engagement shaped this component directly. It guided the focus of the simplified network on the corridors most likely to carry diverted traffic, informed the scenario capacity factors set with BART and Caltrans staff, and motivated the bus-bridging case in Section 6.4. This workflow provides a consistent way to translate engineering-based tunnel performance into transportation-relevant disruption and recovery scenarios that can be compared across different levels of fault displacement.

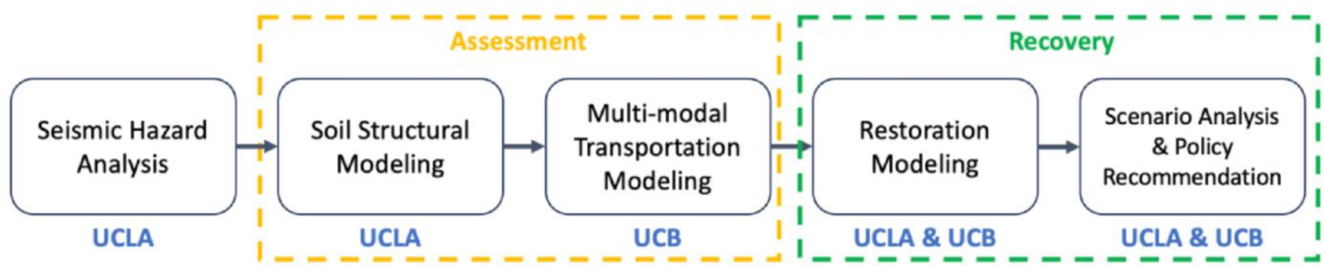

Figure 2. Integrated Assessment–Recovery Workflow.

4 Seismic Performance Analysis of the Berkeley Hills Tunnel

This section introduces the seismic performance analysis of the Berkeley Hills Tunnel conducted by project collaborators at UCLA. This part of the study has been published in a separate report in Zengin et al. (2025), and a summary is included here as a background of the subsequent traffic impact analysis. It provides an overview of the tunnel and demonstrates its expected response to earthquake-induced fault displacement, including resulting damage states, operational constraints, and restoration timelines.

4.1 Overview of the Berkeley Hills Tunnel

The Berkeley Hills Tunnel is a critical BART facility that carries trains between Rockridge and Orinda and provides the only BART rail connection between the inner East Bay and central Contra Costa County. The tunnel opened as part of the Concord line, establishing a high-capacity cross-hills rail link between the inner East Bay and central Contra Costa County.

Earthquakes are the dominant natural hazard for BART infrastructure because they can affect the system through multiple mechanisms, including strong ground shaking, fault rupture, liquefaction, and earthquake-induced landslides (BART, 2022b). In BART's hazard mitigation planning, the Berkeley Hills Tunnel is identified as a critical asset that warrants targeted seismic risk-reduction actions. The mitigation strategy list includes seismic retrofit work specific to the tunnel and actions that range from interim measures to longer-term strategies intended to reduce risk. The plan also identifies broader system initiatives that support tunnel resilience, including incorporation of seismic design criteria into BART facilities standards and continued development of a bypass concept to reduce reliance on a single cross-hills link (BART, 2022b).

4.2 Fault-Displacement Scenarios and Damage Outcomes

The UCLA team models the Berkeley Hills Tunnel as a dual-bore system that intersects the Hayward Fault near the west portal. Reinforced concrete lining properties are explicitly represented to capture damage mechanisms associated with fault displacement. A three-dimensional numerical model is developed and calibrated using observed crack patterns attributed to long-term fault creep. The analysis evaluates a range of fault-displacement scenarios to quantify strain demands, damage progression, and resulting operability impacts. Results indicate a progression from predominantly repairable cracking under smaller displacements to severe damage concentrated near the fault plane under larger displacements, including concrete crushing and loss of structural capacity. These damage outcomes correspond to increasingly restrictive operating conditions and longer restoration durations (**Table 1**). Additional details on the modeling approach and results are documented in the UCLA team's report (Zengin et al., 2025).

Table 1. Fault-Displacement Scenarios and Corresponding Damage, Functionality Impacts, and Restoration Timelines for the Berkeley Hills Tunnel (Adapted from Zengin et al., 2025).

Fault displacement (m)	Return period (years)	Exceedance probability over a 50-year tunnel lifespan	Functionality and Restoration timeline
0.2	327	14%	Structural repairs involve patching the affected areas. Minimal disruption to train operations; realignment and repairs may be completed within 1-4 weeks.
0.5	384	12%	Structural repairs include surface repair, localized concrete replacement, and crack sealing. Temporary speed restrictions or partial closures may be necessary (approximately 3 months).
1.0	500	9.50%	Full or partial tunnel closures likely; considerable disruptions to train operations with complex repair strategies including concrete replacement, installation of additional reinforcements, and possibly precast concrete segment reconstruction (approximately 6 months).
1.5	654	7%	Full tunnel closure expected, major service interruptions with detailed planning for repair execution and alternative routing. Reconstruction strategies involve large-scale reinforcement, complete lining replacement, among other possible actions (12-24 months).

These four return-period scenarios and their functionality and restoration timelines are used directly as scenario inputs in the transportation simulation in Section 6, with the BART Berkeley Hills Tunnel capacity factor scaled accordingly per scenario. The fault-displacement scenarios provide a consistent disruption-and-recovery context against which both the engine-choice analysis (Section 6.3.1) and the per-scenario headline travel-time results (Section 6.3.2) are evaluated.

5 Seismic Performance Assessment of Alternative Cross-Hills Routes

Disruption of BART service through the Berkeley Hills Tunnel is evaluated in a system of alternatives context because cross-hills travel can shift to other corridors when rail service is reduced or unavailable. In the Berkeley Hills corridor, the primary roadway substitutes are SR 24 through the Caldecott Tunnel and local Berkeley Hills roadways (**Figure 3**).

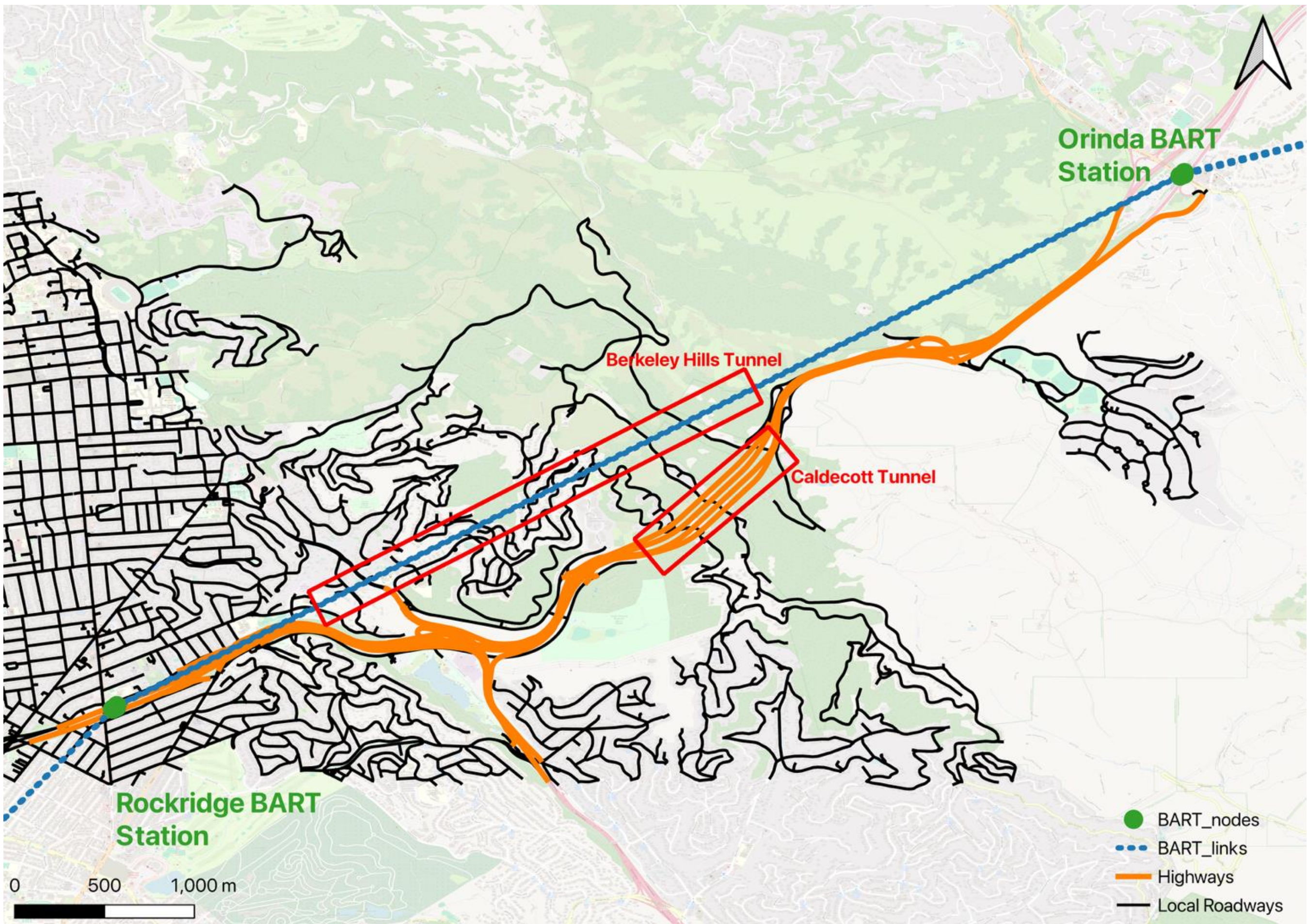

Figure 3. Primary Routes Passing Through the Berkeley Hills.

To support modeling of transportation consequences, the seismic assessment translates earthquake effects on these roadway alternatives into transportation-relevant operability states that can be implemented directly in simulation, including capacity reduction, speed restriction, closure conditions, and a recovery timeline. These roadway states are paired with the rail service states derived from the Berkeley Hills Tunnel seismic analysis so that each earthquake scenario produces a consistent set of time dependent inputs for transportation simulation.

5.1 SR 24 / Caldecott Tunnel

5.1.1 Overview of the Caldecott Tunnel

The Caldecott Tunnel is a primary regional highway facility of SR 24 that connects Oakland and the inner East Bay with Contra Costa County and inland destinations. Under normal conditions, it carries high daily demand. Caltrans reports an annual average daily traffic of 170,000 vehicles for 2023 (Caltrans, 2023). The facility consists of four bores that were constructed in different eras (1937, 1964, and 2013) (Contra Costa Transportation Authority, 2018; Metropolitan Transportation Commission, 2011).

5.1.2 Seismic Damage Assessment for Tunnels

Because the four bores of the Caldecott Tunnel have different design standards and structural details, they may not have the same seismic vulnerability or post-event recovery trajectory. For that reason, a bore specific fragility and recovery characterization would be preferred for this study, particularly given that the Berkeley Hills Tunnel analysis is based on detailed scenario-based modeling by the UCLA team. However, based on consultations with Caltrans engineering staff and a review of publicly available studies, we did not identify a consistent set of bore specific seismic damage and restoration relationships that could be applied across the full earthquake scenario set used in this report. As a result, we assessed the seismic performance of the Caldecott Tunnel using the tunnel fragility and restoration relationships provided in the Hazus Earthquake Model technical guidance (Federal Emergency Management Agency [FEMA], 2024). These relationships provide generalized estimates of damage states, functionality loss, and restoration timing. They are used here to support scenario comparison and are integrated in the regional modeling workflow.

In Hazus, fragility curves relate an earthquake intensity measure to the probability that an asset reaches or exceeds a given damage state (FEMA, 2024). Intensity measures refer to quantitative indicators of earthquake loading or ground movement at a site. In Hazus, these include ground shaking measures, such as peak ground acceleration, and ground failure measures represented by permanent ground deformation (PGD). Peak ground acceleration describes the maximum ground acceleration, while PGD represents earthquake induced ground movement from processes such as liquefaction, landslides, and surface fault rupture (FEMA, 2024). Hazus models these relationships with cumulative lognormal functions defined by a median threshold and a lognormal dispersion parameter, β (FEMA, 2024). In this study, we used the PGD-based formulation to stay consistent with how Hazus represents ground failure related impacts for roadway components.

For tunnels subject to PGD, the probability that a tunnel reaches or exceeds a damage state threshold, ds, is computed as:

$$P(ds \mid PGD) = \Phi\left[\frac{1}{\beta_{ds}} ln\, ln \left(\frac{PGD}{\underline{PGD_{ds}}}\right)\right]$$

Where ds is the defined damage state, $\underline{PGD_{ds}}$ is the median PGD associated with the threshold for damage state ds; β_{ds} is the logarithmic standard deviation for that damage state, and Φ is the standard normal cumulative distribution function (FEMA, 2024).

In this study, the Hazus PGD fragility parameters for the bored or drilled tunnel class are used to estimate exceedance probabilities for the slight, moderate, and extensive or complete damage states (**Table 2**) (FEMA, 2024).

Table 2. Peak Ground Deformation Fragility Function Parameters for Tunnels (FEMA, 2024).

Subcomponent	Damage State	Median (in)	β_{ds}
Bored/Drilled	Slight	6.0	0.7
Bored/Drilled	Moderate	12.0	0.5
Bored/Drilled	Extensive/Complete	60.0	0.5

Figure 4 plots the Hazus PGD fragility functions for the bored or drilled tunnel class using the median thresholds and dispersions in **Table 2**, showing how the probability of reaching or exceeding each damage state increases as permanent ground deformation increases. Each curve represents one damage state exceedance (slight, moderate, and extensive/complete), so the curves provide a depiction of how tunnel damage likelihood transitions from low to high across the range of PGD values (FEMA, 2024).

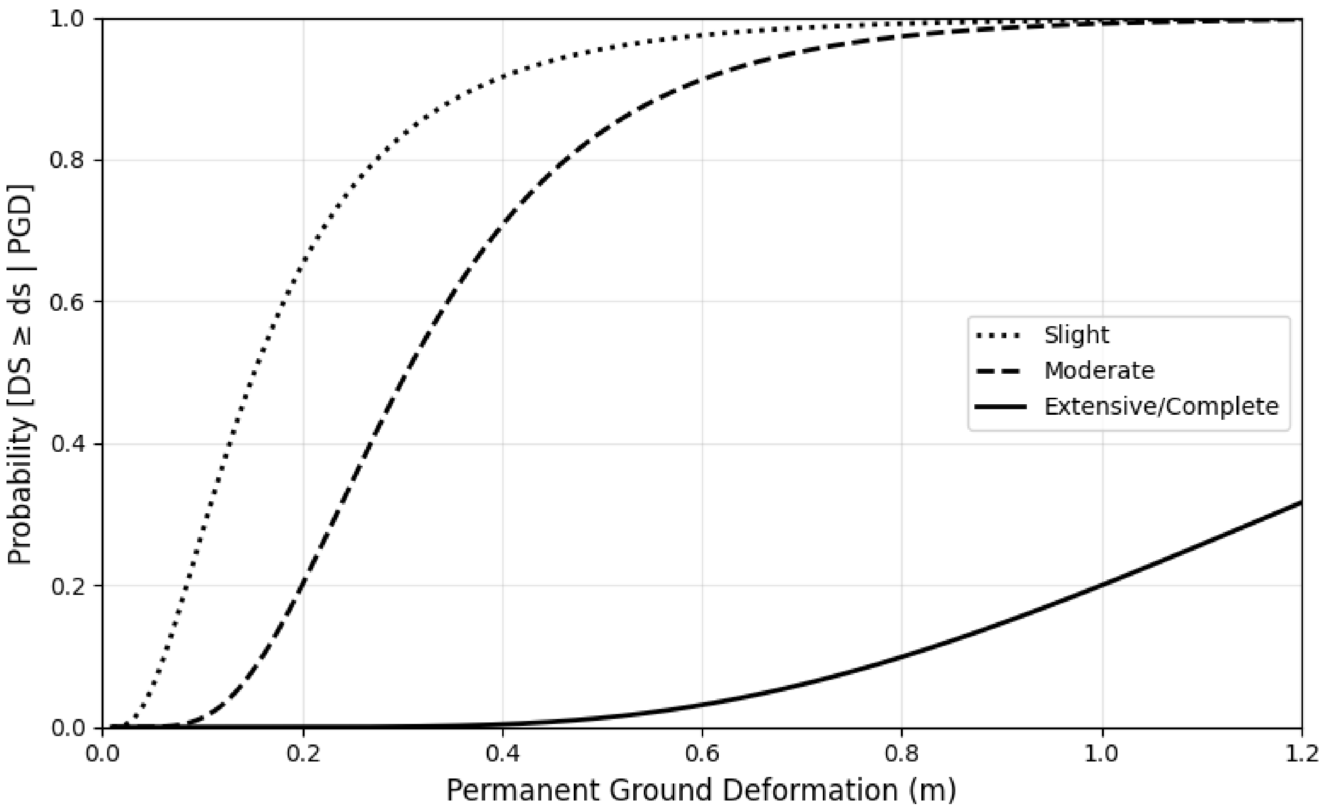

Figure 4. Fragility Curves at Various Damage States for All Types ff Tunnels Subject to Permanent Ground Deformation (Adapted from FEMA, 2024).

Hazus also provides qualitative definitions for these damage states to support interpretation. **Table 3** summarizes the tunnel damage-state descriptions used in this report.

Table 3. Definitions of Damage States for Tunnels (Adapted from FEMA, 2024).

Damage State	Definition
Slight	Minor cracking of the tunnel liner (damage requires no more than cosmetic repair) and some rock falling, or by slight settlement of the ground at a tunnel portal.
Moderate	Moderate cracking of the tunnel liner and rock falling
Extensive	Major ground settlement at a tunnel portal and extensive cracking of the tunnel liner.
Complete	Major cracking of the tunnel liner, which may include possible collapse.

5.1.3 Hazus Restoration Functions for Tunnels

To translate damage into operability during recovery, Hazus provides restoration and functionality relationships that describe the expected fraction of functionality over time following an event (FEMA, 2024). In this study, we represented restoration using the discretized tunnel functionality values provided by Hazus (**Table 4**). We use the discretized form to align with the time-step structure of the scenario-based transportation simulation and because stakeholder input suggests that actual operations may involve staged reopening and partial service restoration that depends on inspection outcomes and operational decisions. Consistent with the broader approach to the Caldecott Tunnel inputs in this study, these restoration relationships are interpreted as screening-level assumptions that can be updated if tunnel-specific recovery information becomes available.

Table 4. Discretized Restoration Functions for Tunnels (FEMA, 2024).

Classification	Damage State	Functional Percentage (%)				
		1 Day	3 Days	7 Days	30 Days	90 Days
Tunnels	Slight	90	100	100	100	100
Tunnels	Moderate	25	65	100	100	100
Tunnels	Extensive	5	8	10	30	95
Tunnels	Complete	0	3	3	5	15

5.1.4 Regional Resilience Determination (R2D)

We implemented the Hazus-based fragility and restoration relationships within the Natural Hazards Engineering Research Infrastructure (NHERI) SimCenter Regional Resilience Determination (R2D) workflow, which supports regional infrastructure performance assessment and can propagate uncertainty through simulation-based methods (McKenna et al., 2025). For consistency with the Berkeley Hills Tunnel scenario set, we use the same earthquake scenarios to define hazard inputs for the Caldecott Tunnel analysis and apply the Hazus tunnel fragility relationships to estimate damage-state probabilities from PGD. R2D then assigns tunnel damage states for each scenario and maps those states to time-dependent functionality using the Hazus restoration relationships. These functionality trajectories subsequently can be converted to capacity multipliers that serve as time-dependent inputs to the transportation simulation (FEMA, 2024; McKenna et al., 2025).

5.1.5 Caldecott Tunnel Damage-State Estimates

Table 5 summarizes the Caldecott Tunnel damage-state assignments estimated by R2D for different earthquake scenarios at the immediate post-event condition. Recovery-stage functionality for each damage state is then represented using the corresponding restoration functions in **Table 4**.

Table 5. Estimated Damage Levels for the Caldecott Tunnel Immediately After the Earthquakes.

Return period (years)	Damage State
327	1
384	2
500	2
654	3

5.2 Cross-Hills Local Roads

5.2.1 Overview of the Cross-Hills Local Roads

Local roads in the Berkeley Hills provide additional cross-hills connectivity, but they are generally low-capacity facilities with limited redundancy. Field observations and stakeholder discussions indicate that many segments are two-lane, curvilinear hillside roadways with constrained geometry and limited ability to accommodate large diversion volumes during major disruptions. From an earthquake consequence perspective, these roads are also exposed to geotechnical ground-failure processes that can reduce operability by creating pavement offsets, settlement, or localized blockage.

5.2.2 Seismic Damage Assessment of the Roadways

Given current data constraints for site-specific slope inventories and geotechnical characterization in this phase, roadway damage is estimated using the NHERI SimCenter R2D workflow (McKenna et al., 2025). In the current implementation, roadway impacts are driven by permanent ground deformation associated with liquefaction-related surface manifestations, including lateral spreading and vertical settlement, following the ground-deformation relationships implemented in R2D and attributed to Wang et al. (2021). Compared with Hazus's generalized fragility functions, the Wang et al. approach used in R2D links roadway damage more directly to spatially varying permanent ground deformation fields, enabling a more location-specific representation of liquefaction-driven roadway impacts within the regional simulation workflow (McKenna et al., 2025; Wang et al., 2021).

However, because the R2D roadway module focuses on liquefaction-related ground deformation (Wang et al., 2021), it does not explicitly represent landslides or broader slope-instability mechanisms that can be important in steep terrain. This limitation is particularly relevant for hillside roads, where landslide-induced closure and debris impacts may govern operability in some scenarios. As a result, local-road disruption may be understated in cases where slope instability dominates the hazard environment.

For interpretability and consistency across lifeline components in this report, roadway damage states are described using Hazus damage-state terminology and definitions (**Table 6**) (FEMA, 2024).

Table 6. Definitions of Damage States for Roads (Adapted from FEMA, 2024).

Damage State	Definition
Slight	Slight settlement (a few inches) or offset of the ground
Moderate	Moderate settlement (several inches) or offset of the ground
Extensive	Major settlement of the ground (a few feet)
Complete	Major settlement of the ground (i.e., same as Extensive damage)

5.2.3 Hazus Restoration Functions for Roadways

To estimate recovery-stage operability, we used the Hazus restoration and functionality relationships that describe expected functionality over time following an event (FEMA, 2024). In this study, we used the discretized roadway functionality values provided by Hazus for highway system roadways as a consistent, scenario-based representation of restoration trajectories (**Table 7**). These values are treated as planning assumptions that support time-dependent capacity inputs in the transportation simulation and can be refined as more detailed roadway-specific recovery information becomes available.

Table 7. Discretized Restoration Functions for Highway System Roadways (FEMA, 2024).

Classification	Damage State	Functional Percentage (%)				
		1 Day	3 Days	7 Days	30 Days	90 Days
Roadways	Slight	90	100	100	100	100
Roadways	Moderate	25	65	100	100	100
Roadways	Extensive/ Complete	10	14	20	70	100

5.2.4 Local Road Damage and Functionality Estimates

Liquefaction susceptibility in the Berkeley Hills is generally limited compared with low-lying Bay Area soils. Consistent with this setting, the liquefaction-driven permanent ground deformation mechanism represented in R2D indicates that most local-road segments remain intact, with only a small number of links assigned minor damage that is expected to be restored quickly. However, because this phase of the study does not include landslide-related blockage and slope-failure mechanisms, local-road impacts may be underestimated in scenarios where slope instability governs roadway operability.

6 Transportation Impact Assessment for Berkeley Hills Tunnel Disruption

This section evaluates how disruption of BART service through the Berkeley Hills Tunnel affects cross-hills mobility during both the immediate disruption period and the recovery stage. Building on the engineering-based tunnel functionality and restoration scenarios from the UCLA structural analysis, and the alternative route operability states estimated for SR 24 through the Caldecott Tunnel and for cross-hills local roads, we translate time dependent infrastructure conditions into network capacity inputs and simulate resulting system performance. The objective is to provide a scenario-based consequence assessment approach that links infrastructure damage and recovery assumptions to practitioner relevant outcomes, including travel time, rerouting pressure on substitutes, and the sensitivity of results to key behavioral and operational assumptions.

6.1 Transportation Simulation Platform and Modeling Approach

6.1.1 Transportation Simulation Developed in RIMI Phase 1

Transportation consequences are evaluated using the transportation simulation platform developed in UC ITS RIMI Phase 1, which integrates an agent-based roadway model and an agent-based metro system simulator for post-earthquake planning applications (Soga et al., 2024). The roadway component is implemented as a semi-dynamic traffic assignment model with residual demand. This design supports large-scale, repeated scenario evaluation at manageable computational cost while still capturing plausible congestion responses to closures, capacity reductions, and recovery-stage changes in facility operability (Soga et al., 2024). The metro component is General Transit Feed Specification (GTFS) compatible and supports scenario-based edits to the transit network, including station outages and segment closures, while representing traveler, train, and platform interactions at fine temporal resolution (Soga et al., 2024).

At the multimodal level, the platform combines OpenStreetMap roadway networks and GTFS transit networks into a unified routing environment and evaluates system performance at sub-hourly time steps. Route planning is implemented using a shortest-path procedure based on estimated travel times, with the simplifying assumption that each agent selects the minimum travel-time path given prevailing network conditions and the current scenario inputs. The platform records agent-level outcomes such as travel time and fare, enabling consistent comparison across baseline, disruption, and recovery cases with different capacity constraints and operating assumptions (Soga et al., 2024).

6.1.2 Traffic Assignment Methods

This case study uses two route-assignment engines for the traffic network. A quasi-equilibrium engine inherited from RIMI Phase 1 supports scenario-based screening at low computational cost, and a user-equilibrium engine is introduced in this study to provide a stabilized routing baseline for recovery-stage interpretation (Soga et al., 2024). Both engines share the same link cost specification, so that any differences in results are isolated to the assignment behavior itself.

The quasi-equilibrium engine treats traffic as piecewise static within each time step, holding link travel times fixed and assigning every traveler departing within the step to the estimated minimum-travel-time path on an all-or-nothing basis (Soga et al., 2024); travel times update between steps as flows change. This avoids the iterative network equilibrium solve at each recovery time point and is well suited to large scenario sweeps in city-scale networks with many substitute routes. In a corridor-scale network with only a few feasible cross-hills routes under severe disruption, however, the all-or-nothing treatment can understate sustained congestion, so the analysis is supplemented with a user-equilibrium engine and the two are compared empirically in Section 6.3.1.

The user-equilibrium engine assigns flow according to Wardrop's first principle: at equilibrium, no traveler can reduce travel time by unilaterally changing routes given the prevailing congestion pattern (Wardrop, 1952). Equilibrium is reached by Frank-Wolfe iteration over the routing graph until path costs satisfy the Wardrop condition to a specified tolerance (LeBlanc et al., 1975). In this case study, the simplified cross-hills network forces diverted trips onto a limited set of alternatives, so assignment assumptions strongly affect how congestion and detours are distributed across routes; the user-equilibrium engine is applied as a comparative modeling layer in recovery-stage experiments to provide a stabilized routing baseline against which the quasi-equilibrium results can be interpreted (Section 6.3.1).

Both engines use the standard Bureau of Public Roads link-performance function (Federal Highway Administration convention; Sheffi, 1985) to relate flow to loaded travel time. For each link, the loaded travel time t is computed as:

$$t = t_0 \left(1 + \alpha \left(\frac{v}{c}\right)^{\beta}\right)$$

Where t_0 is the free-flow travel time of the link, v is the link flow, c is the link capacity, and α and β are dimensionless parameters set to the standard BPR values of 0.15 and 4 (Sheffi, 1985). Because this function increases with the fourth power of the volume-to-capacity ratio, under extreme oversaturation (a volume-to-capacity ratio well above one) it returns very large travel-time values that indicate the degree of network stress rather than literal trip durations; such values appear in the severe-disruption results that follow and are interpreted on that basis (Sections 6.3.3 and 6.4).

6.2 Transportation Simulation Inputs

6.2.1 Road Network

The roadway network was extracted from OpenStreetMap and processed using OSMnx (Boeing, 2017). The resulting network provides link level attributes needed for simulation, including segment length, connectivity, and baseline operating characteristics. To focus the analysis on cross-hills travel and the primary substitutes to BART service through the Berkeley Hills Tunnel, the roadway network was spatially subset to the Berkeley Hills study area rather than representing the full Bay Area roadway system.

For this case study, the subset network was further simplified to a small set of representative cross-hills corridors, consistent with stakeholder input that emphasized focusing on the primary routes most likely to carry diversion during disruption. This additional simplification also reduces modeling complexity and computational burden, enabling clearer interpretation of how scenario-based capacity and operability changes affect rerouting and travel time. The simplified network includes SR 24 through the Caldecott Tunnel and selected local road routes across the hills (**Figure 5**). Together with connecting boundary nodes on either side of the East Bay barrier and a BART rail link representing service through the Berkeley Hills Tunnel, the simplified network covers three primary cross-hills auto corridors (SR 24 through the Caldecott Tunnel, Mountain Road, and Claremont Avenue) and provides the topology used by the routing algorithms in Section 6.1.

Operational parameters were assigned using lane counts and facility type. Free flow conditions and baseline capacities were informed by standard highway design and operations references (American Association of State Highway and Transportation Officials, 2018; Transportation Research Board, 2022). Scenario specific capacity reductions were then implemented as link level effective capacity multipliers to represent throughput limitations associated with inspections, lane closures, speed restrictions, and other post-earthquake operating constraints.

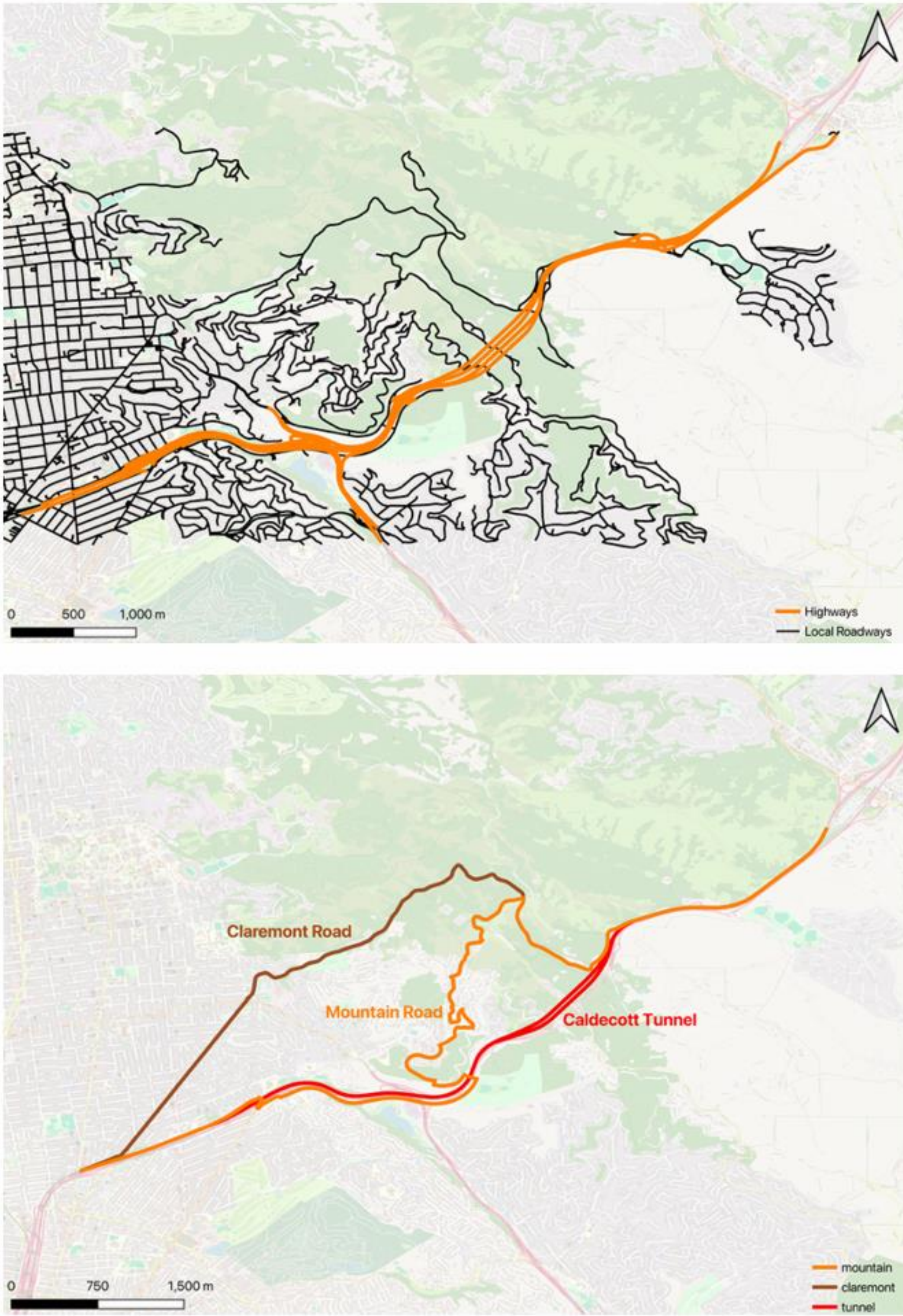

Figure 5. Road Network Simplification.

6.2.2 BART Network

Rail inputs were derived from BART's GTFS schedules, which provide station sequences, scheduled travel times, and service structure for the Orinda-Rockridge segment that passes through the Berkeley Hills Tunnel (BART, 2025). These schedules were loaded into the agent-based metro simulator developed in RIMI Phase 1 (Soga et al., 2024), which is GTFS compatible and supports scenario-based modifications to the transit network, including segment closures and service changes. The simulator advances passenger agents through scheduled trains while applying capacity constraints and segment-level operating states, so disruption scenarios that change BART's effective service availability or headway translate directly into changes in agent travel time through the affected segment.

6.2.3 Capacity Inputs

For roadway facilities, earthquake impacts were represented by mapping estimated damage states to functionality levels and then treating functionality as a proxy for usable traffic capacity. Specifically, the Hazus Earthquake Model (the Federal Emergency Management Agency's standardized methodology for estimating earthquake damage and functionality loss to physical infrastructure) is used as the basis for translating engineering damage estimates into transportation-relevant operating conditions. Tunnel damage states from this methodology were converted to immediate post-event functionality percentages using the Hazus transportation functionality and restoration relationships (FEMA, 2024). The resulting functional percentage was applied as an effective capacity multiplier for the Caldecott Tunnel links and the selected cross-hills local roadways. This mapping is intended to represent functionality reductions that may occur even without full closure, such as lane restrictions, speed management, inspection requirements, and repair activity. Recovery stage capacity was represented by updating functionality over time using the assumed restoration trajectories provided in Hazus (FEMA, 2024).

For BART service through the Berkeley Hills Tunnel, capacity effects were derived from the scenario-based restoration timelines based on the UCLA assessment (Zengin et al., 2025). Qualitative operating conditions, including minimal disruption, speed restriction or partial closure, likely closure, and full closure, were translated into capacity factors through discussion with the relevant stakeholders. These factors represent the fraction of normal tunnel train throughput expected under each scenario in the immediate post-event period. **Table 8** summarizes the capacity factors applied immediately after the earthquake for the case study scenarios.

Table 8. Traffic Capacity Factors Used for Scenario Analysis Immediately After the Earthquakes.

Return period (years)	Berkeley Hills Capacity	Caldecott Tunnel Capacity	Local Road Capacity
327	90%	90%	90%
384	50%	25%	90%
500	25%	25%	90%
654	~0%	~0%	90%

While the case study results in Section 6.3 use the immediate post-event capacity factors in **Table 8**, the model is designed to support analysis at any time point along the restoration curve. Substituting the corresponding restoration-stage capacity values from the discretized restoration functions in **Table 4** and **Table 7** (and from the per-scenario restoration timelines in **Table 1**) allows the same simulation to be evaluated at later time horizons (e.g., one week, one month, or three months post-event), so stakeholders can compare mobility outcomes and mitigation effectiveness at different stages of recovery and identify the time horizons over which different operational strategies are most binding.

6.2.4 Travel Demand

Travel demand inputs specify origin, destination, departure time, and travel mode for each agent. For the BART system, demand was derived from BART ridership reports, which includes origin-destination data based on faregate entries and exits data (BART, 2025). To estimate passenger volumes that traverse the Berkeley Hills Tunnel, we use a segment-based aggregation approach: a trip is counted as tunnel-crossing when its origin station and destination station lie on opposite sides of the Orinda–Rockridge segment, implying that the trip must pass through the tunnel. This method was applied to 2024 weekday hourly ridership data to generate time-of-day tunnel-crossing demand profiles (BART, 2025). Application of this method yields approximately 5,361 westbound and 585 eastbound tunnel-crossing passenger-trips during the 7–8 AM weekday peak hour, which sets the baseline rail demand used in the simulation experiments and in the bus-bridging case in Section 6.4.

For roadway demand, baseline volumes were derived from Caltrans traffic count products, including annual average daily traffic summaries for SR 24 and related facilities (Caltrans, 2023). These counts were used to estimate cross-hills roadway demand under normal conditions. The Caldecott Tunnel on SR 24 carries an annual average daily traffic of approximately 170,000 vehicles and a peak-hour volume of approximately 13,000 vehicles (Caltrans, 2023). Aggregating SR 24 with the secondary cross-hills corridors (Mountain Road and Claremont Avenue) and applying a westbound-dominant AM peak directional split yields a baseline cross-hills auto demand of approximately 15,000 westbound vehicles during the 7–8 AM weekday peak hour, which sets the baseline roadway demand used in the simulation experiments and in the bus-bridging case in Section 6.4.

Because this case study focuses on cross-hills movement rather than full regional circulation, agent origins and destinations were assigned to boundary nodes on either side of the study area. Origins and destinations were selected to reflect travel direction and mode, so that simulated trips represent cross-hills travel demand that would plausibly use the Berkeley Hills Tunnel and its primary roadway alternatives.

Recovery-stage travel demand is uncertain, and predicting post-event mode choice and trip suppression is beyond the scope of this study. We therefore treat the recovery-stage demand level as a scenario parameter rather than a fixed input. The per-scenario results in Section 6.3.2 use a single representative level, and the model can be re-run at any specified value.

6.3 Transportation Simulation Results

We ran the full set of disruption and recovery scenarios described in the previous sections. To keep the discussion focused, this section presents only representative results that illustrate the main performance patterns and modeling insights. The full scenario set can be reproduced from the simulation code, the network and demand inputs, and the analysis scripts, which are openly available at https://github.com/cb-cities/berkeley-hills-tunnel.

6.3.1 Traffic Assignment Engine

Section 6.1.2 motivated the user-equilibrium engine on theoretical grounds, noting that the quasi-equilibrium engine's within-step all-or-nothing assignment is poorly suited to a corridor-scale network with only a handful of feasible routes. This subsection confirms the engine choice empirically by running both engines on the same simplified cross-hills topology under two representative conditions: baseline operations and the severe-disruption 654-year scenario at demand set to 25 percent of normal. The comparison is restricted to the roadway network to exclude BART waiting-time effects and isolate differences in route allocation and congestion formation.

summarizes results for two representative conditions: baseline operations and a severe-disruption scenario immediately following an earthquake corresponding to a 654-year return period, with cross-hills demand suppressed to 25 percent of normal. Under baseline conditions, we assign 15,000 roadway trips within a one-hour morning peak period. The quasi-equilibrium assignment produces an average cross-hills travel time of 14.0 minutes, compared with 23.2 minutes under the user-equilibrium assignment. Under the severe disruption scenario, the user-equilibrium assignment captures the expected deterioration in performance, with average travel time rising to 41.4 minutes. The quasi-equilibrium assignment, however, produces a low value of 5.3 minutes for the same scenario.

Table 9 summarizes results for two representative conditions: baseline operations and a severe-disruption scenario immediately following an earthquake corresponding to a 654-year return period, with cross-hills demand suppressed to 25 percent of normal. Under baseline conditions, we assign 15,000 roadway trips within a one-hour morning peak period. The quasi-equilibrium assignment produces an average cross-hills travel time of 14.0 minutes, compared with 23.2 minutes under the user-equilibrium assignment. Under the severe disruption scenario, the user-equilibrium assignment captures the expected deterioration in performance, with average travel time rising to 41.4 minutes. The quasi-equilibrium assignment, however, produces a low value of 5.3 minutes for the same scenario.

Table 9. Average Cross-Hills Travel Time, Quasi-Equilibrium versus User-Equilibrium Assignment (Roadway Network Only).

Return period (years)	Travel Demand	Quasi-equilibrium (min)	User-Equilibrium (min)
0 (Baseline)	100%	14.0	23.2
654	25%	5.3	41.4

For the quasi-equilibrium model, demand is assigned in short intervals (10 minutes) with link volumes reset each interval, so all-or-nothing routing loads the corridor with the shortest estimated travel time, and diverts to an alternate in the next interval, returning the interval after in this case study. With only a couple of viable alternates, this oscillation gives each corridor alternating intervals to clear its load; congestion builds within an interval but is spread across corridors and time, under-representing the sustained oversaturation a near-total Caldecott closure should produce.

This is expected behavior for interval-based all-or-nothing assignment. The engine remains appropriate for large networks with many routes but may not be suitable in this corridor-scale, severely disrupted case, where the network reduces to a few alternates. The user-equilibrium engine instead holds all flow in a single equilibrium (Wardrop, 1952; Sheffi, 1985), yielding 41.4 minutes, and is therefore adopted for the per-scenario analysis and all subsequent results. Computational cost is not a constraint at this scale, requiring 1.1 seconds for the quasi-equilibrium engine and 13.7 seconds for the user-equilibrium engine on the simplified network.

6.3.2 Per-Scenario Travel-Time Results

This section presents one set of simulation results across the four scenarios to illustrate the model's outputs. Cross-hills demand is set to 25 percent of normal as a representative recovery-stage level, with its influence on the results examined in Section 6.3.3. The four scenarios were run with the user-equilibrium engine on the simplified topology. BART tunnel-crossing travel time was estimated with the RIMI Phase 1 agent-based metro simulator (Soga et al., 2024), which advances passenger agents through BART's Yellow-line GTFS schedule (BART, 2025), with each scenario's capacity factor applied to the 10-minute peak headway by inverse-headway scaling. In-vehicle time and per-train capacity were held at nominal values (5.87 minutes for the Rockridge to Orinda segment; about 1,000 passengers per ten-car train at crush load), and the simulator computed wait and travel time from boarding and train-propagation dynamics. Per-train load stays below the maximum capacity at the 327-, 384-, and 500-year scenarios, so all rail demand remains on BART; at the 654-year scenario BART has no service and we assume that demand shifts to auto. The simulation results are reported in **Table 10**.

Table 10. Mean Cross-Hills Travel Time per Scenario, by Mode and Overall (User-Equilibrium Engine; Recovery-Stage Demand at 25 Percent of Normal; AM Peak, Westbound).

Return period (years)	Car	BART	Overall (passenger-weighted)
327 (mild)	8.1 min	11.4 min	9.0 min
384	22.0 min	15.9 min	20.4 min
500	22.0 min	25.9 min	23.0 min
654 (severe)	41.4 min	(no service)	41.4 min

Both modal travel times deteriorate as damage severity increases. Car time rises as Caldecott Tunnel capacity falls, and BART time rises as the effective headway lengthens under the scenario capacity factors, until BART service ceases entirely at the 654-year scenario, where the displaced rail demand joins the cross-hills auto demand and overall travel time reaches 41.4 minutes. The overall value in each scenario is the passenger-weighted blend of the two modal times given the rail and auto shares, and it depends on how travelers are assumed to split between modes. At the 327-, 384-, and 500-year scenarios the model holds all rail demand on BART, an upper bound on BART utilization; if riders instead abandoned BART under long waits, such as the 40-minute headway at the 500-year scenario, the displaced demand would shift to auto and raise the auto and overall times. At the 654-year scenario the model assigns all displaced rail demand to auto, a worst case for the road network because it loads the alternates with the maximum possible diversion. This assignment is also a simplification, since transit-dependent riders without a personal vehicle could not drive and would instead rely on substitutes such as a bus bridge or ride-hail, an equity consequence discussed in Section 7.2. The 654-year scenario is examined further as the bus-bridging case in Section 6.4.

6.3.3 Sensitivity Analysis of Demand

The 25-percent recovery-stage demand level used for the per-scenario results in Section 6.3.2 is a representative choice rather than a measured value, so its influence on those results is tested directly. The 384-year scenario is used for this test because its mid-range capacity impacts produce the most informative gradient. At the 327-year scenario the impacts are mild, while at the 654-year scenario the system is saturated regardless of demand and the gradient collapses. The user-equilibrium engine was rerun at four recovery-stage demand levels (25, 50, 75, and 100 percent of normal), with the **Table 8** capacity factors held fixed and the same Frank-Wolfe convergence criterion used elsewhere in this section.

Table 11. Sensitivity of Mean Cross-Hills Travel Time to Recovery-Stage Demand at the 384-Year Scenario (User-Equilibrium Engine; Table 8 Capacity Factors Held Fixed; AM Peak, Westbound).

Recovery-stage demand	Car	BART	Overall (passenger-weighted)
25% (Section 6.3.2 baseline)	22.0 min	15.9 min	20.4 min
50%	29.5 min	15.9 min	25.9 min
75%	74.2 min	26.1 min	61.6 min
100%	196.5 min	39.9 min	155.2 min

The analysis shows that cross-hills travel times are highly sensitive to the assumed recovery-stage demand. With the capacity factors held fixed at their 384-year values, mean travel times rise sharply in both modes as demand increases from 25 toward 100 percent of normal, so results based on 25-percent demand would substantially understate cross-hills travel time if the realized demand were higher. BART per-train load reaches roughly 894 passengers at 50-percent demand, just below the 1,000-passenger maximum capacity. At higher demand the trains run full, and the passengers who cannot board wait for later trains, so the mean BART time rises from 15.9 minutes to 26.1 minutes at 75 percent and 39.9 minutes at 100 percent. On the roadside, the car time reaches 74.2 and 196.5 minutes at the same levels, Bureau of Public Roads outputs at volume-to-capacity ratios well above one that indicate network stress rather than literal trip durations.

These runs vary recovery-stage demand alone; the capacity factors and the behavioral mode choice are held fixed. In practice, passengers may shift modes or trip times under the long auto travel times that arise at 75 and 100 percent demand. The values reported here therefore bound the screening-level response of the simulation model to the demand assumption, not the realized post-earthquake travel-time distribution.

6.4 Bus-Bridging Mitigation: A Representative Case

As an extension of the model, this section presents a representative case demonstrating how mitigation strategies can be evaluated within the simulation environment. The case examines bus bridging, a temporary roadway service connecting the two BART portal-side stations, under the 654-year scenario, in which BART rail service through the Berkeley Hills Tunnel is fully unavailable. Demand is held at the same 25 percent recovery-stage level used for the per-scenario results in Section 6.3.2. Two extreme cases bracket the realistic policy space: in Case ON, an unconstrained bus service carries all displaced rail riders, with the buses themselves running on the cross-hills alternates; in Case OFF, all displaced riders drive as single-occupancy vehicles. Real-world outcomes sit between these bookends.

At 25 percent recovery-stage demand, about 3,750 cars and about 1,340 displaced rail riders seek to cross. In Case OFF all of them are on the road, about 5,090 vehicles, producing a mean cross-hills car travel time of 41.4 minutes, the same value reported for the 654-year scenario in **Table 10**. In Case ON the displaced riders move to the bus bridge. Carrying about 1,340 riders at about 50 passengers per bus, consistent with the capacity of a standard 40-foot transit coach, requires roughly 27 bus-trips, which at about 3 passenger car equivalents per bus on these grades add about 80 passenger car equivalents to the local-road alternates that the buses must use, because the Caldecott Tunnel is closed at this scenario. Because the two cases are constructed as bracketing extremes, the simulation counts only on-road vehicle travel time and ignores the bus wait time, boarding and dwell time, and the transfer and access times that displaced riders would actually experience on the bus bridge; the reported Case ON figure is therefore a road-network travel time, not a door-to-door bus journey time. The user-equilibrium engine returns a mean cross-hills car travel time of about 28.6 minutes for Case ON, a reduction of about 12.8 minutes, or 31 percent, relative to Case OFF, alongside a roughly 25 percent reduction in road loading (**Table 12**).

Table 12. Cross-Hills Travel Time and Loading at the 654-Year Scenario During Recovery (25 Percent Recovery-Stage Demand), with and without Bus-Bridging Mitigation (User-Equilibrium Engine, AM Peak Westbound; Loading in Passenger Car Equivalents).

Case	Cross-hills loading (passenger car equivalents)	Mean cross-hills car travel time (min)
Case OFF (no bus bridge)	5,090	41.4
Case ON (bus bridge)	3,830	28.6
Change	−1,260 (−25%)	−12.8 min (−31%)

Operating a bus bridge across these roads is itself uncertain even at this recovery-stage service level. At the 654-year scenario the Caldecott Tunnel is closed, so buses cannot use SR 24 and have to run on the same two-lane, curving hillside roads. Those grades slow buses and enlarge their road-space footprint, narrow alignments leave little room for stops, staging, or passing, and local-road operability could be worse than modeled because landslide and slope-failure blockage is not represented in this phase. The recovery-stage service of about 27 buses per hour, roughly one every two minutes, is operationally plausible, but the driver, vehicle, and cross-jurisdiction constraints still apply, so the modeled relief is an upper bound that an actual bus bridge would fall short of.

6.4.1 Behavioral Assumption for the Bus-Bridging Case

The model supports multimodal simulation, and a complete mitigation evaluation would model the mode-choice behavior of displaced passengers as a function of post-disruption travel time, fare, wait, and access conditions. Mode choice under normal conditions is well established in the discrete-choice literature (McFadden, 1974; Ben-Akiva & Lerman, 1985; Train, 2009). Mode choice in the hazard context is far less developed, because service is degraded, information is incomplete, and behavior may diverge sharply from equilibrium expectations. Empirical work on transit strikes and other closure natural experiments shows that observed behavior often departs substantially from logit-model predictions, with habit and information effects playing a larger role than in equilibrium settings (Anderson, 2014; Larcom et al., 2017; Pel et al., 2012). Because the hazard-context behavioral literature is sparse, the representative case adopts a deterministic mode-substitution assumption rather than behavioral parameters that cannot be reliably calibrated to a post-earthquake setting. The operational feasibility of a bus bridge and its distributional value for transit-dependent riders are discussed further in Sections 7.1 and 7.2.

6.5 Uncertainty Quantification

Post-earthquake link capacities and recovery-stage demand are both highly uncertain, and because the travel-time response is nonlinear, a single estimate run reveals neither how widely the outcome can vary nor which inputs control it. This section addresses both at the 500-year scenario on the roadway network. Forward propagation quantifies the spread in cross-hills travel time under uncertain capacity (Section 6.5.1), and a variance-based decomposition ranks the inputs that drive it (Section 6.5.2).

6.5.1 Forward Propagation with Latin Hypercube Sampling

We represented the two cross-hills capacity multipliers, SR 24 through the Caldecott Tunnel and the local-road alternates, as lognormal random variables centered on their Hazus recovery-stage values (about 0.32 and 0.87 at the 500-year early-recovery horizon), and propagated them with 200 Latin hypercube samples, holding demand at 25 percent of normal and solving each sample by user-equilibrium assignment (quoFEM and Dakota; McKenna et al., 2025).

At the central inputs the model returns about 17 minutes, essentially the mean of the resulting distribution (**Figure 6**). The distribution is right-skewed and bimodal, spanning roughly 9 minutes when the sampled Caldecott capacity carries cross-hills traffic to 32 minutes when it does not and flow diverts to the local roads (mean 17.0, median 16.5, 95th percentile 24.1, maximum 31.6). Under unfavorable capacity realizations, travel time can nearly double the central estimate, so recovery planning should account for this downside rather than the average alone.

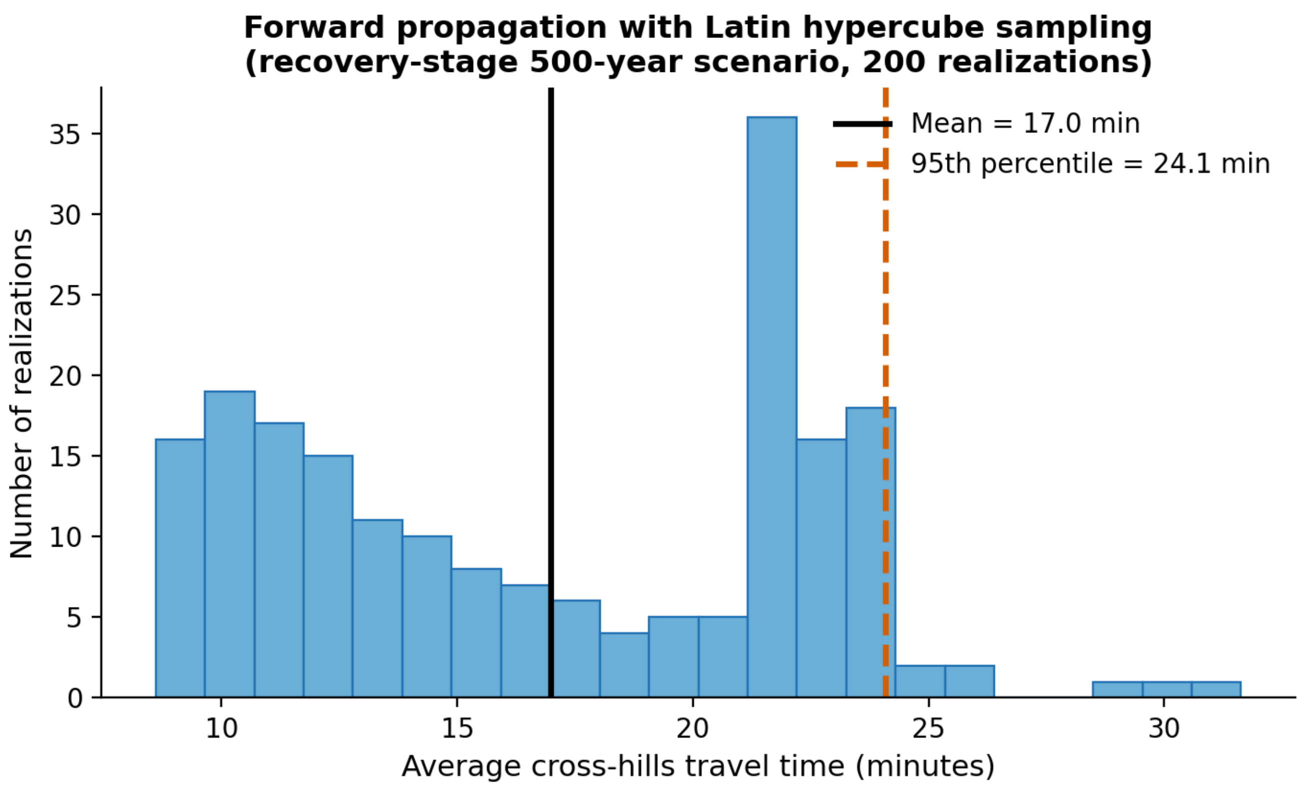

Figure 6. Average Cross-Hills Travel Time Under Recovery-Stage Capacity Uncertainty at the 500-Year Scenario (200 Latin Hypercube Realizations; Mean 17.0 Minutes, 95th Percentile 24.1 Minutes).

6.5.2 Variance-Based Sensitivity Decomposition

To identify which inputs contribute most to this variation, we computed Sobol indices (quoFEM and Dakota, 500 base samples) over recovery-stage demand and the eight individual cross-hills links (C1 through C8, **Figure 7**), refining the two aggregate capacity groups used above to the link level and adding demand. Recovery-stage demand dominates, with main and total indices of about 0.70 and 0.74 (**Figure 8**). Among the links, the Caldecott Tunnel segment C3 leads at about 0.13 main and 0.16 total, followed by the eastern approach C1 at 0.08 and 0.12. The local roads and the remaining links are negligible.

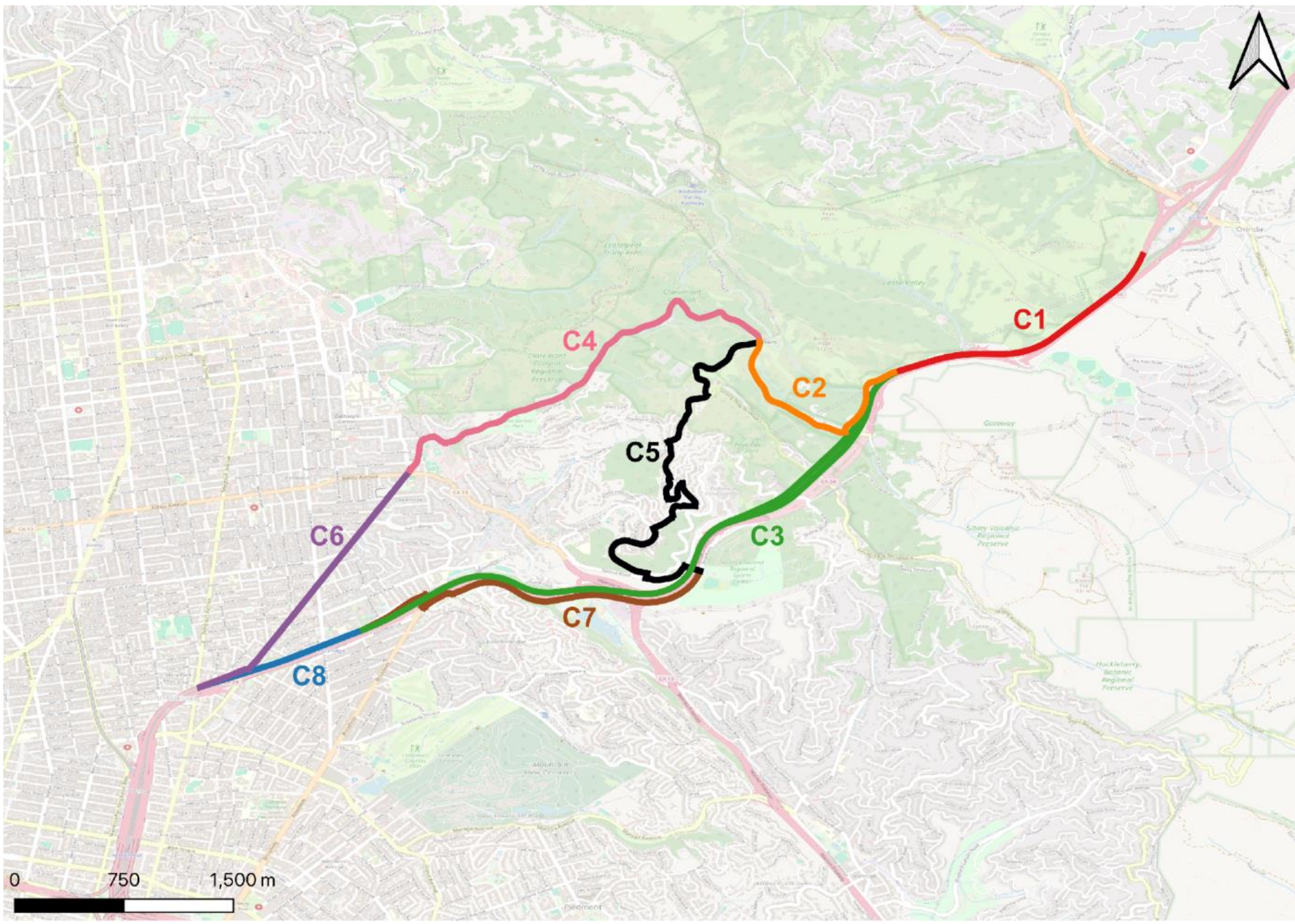

Figure 7. Cross-Hills Road Network Links (C1 Through C8) Used in the Uncertainty and Sensitivity Analysis.

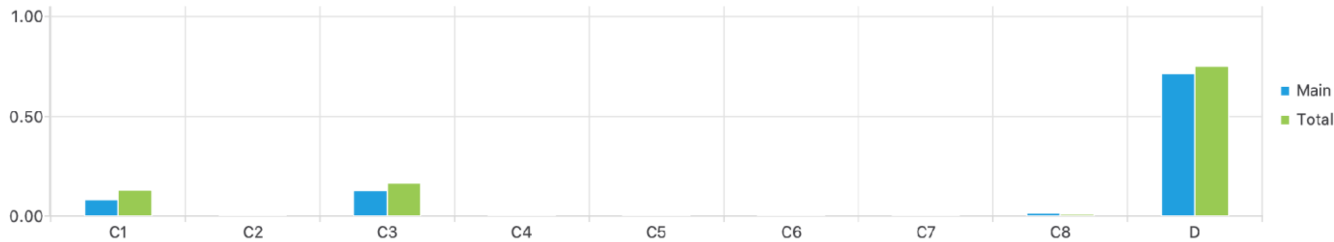

Figure 8. Sobol Main-Effect and Total-Effect Indices for the Cross-Hills Link Capacities.

These results show which factors deserve the more attention in recovery-stage planning and where bottlenecks are most likely to form. Recovery-stage demand has the largest effect, reinforcing the demand sensitivity in Section 6.3.3 and pointing to travel-demand management as a key response. Among the physical road sections, the Caldecott Tunnel segment C3 has the greatest influence on cross-hills travel time while the tunnel remains in service, making it the bottleneck to watch most closely; the shared eastern approach C1 is a secondary concern because every route depends on it. The local roads register as negligible here only because the Caldecott Tunnel is still partially functional and carries most of the traffic, leaving the local roads lightly loaded. Were the tunnel more heavily damaged or fully closed, diverted demand would shift onto these local roads, making their capacity and recovery critical to cross-hills travel time, so route-specific assessment of them under the severe scenarios would improve the accuracy of the results. Finally, because the indices depend on the assumed input ranges and on an assumption of independent ground motion across links, they are best interpreted as relative contributions rather than precise shares.

7 Discussion

7.1 Recovery Process and Operational Strategy

This study focuses on the recovery stage, when facility functionality changes over time and travelers adjust to evolving constraints. The recovery timelines were developed jointly by the geotechnical earthquake engineering and transportation researchers and informed by stakeholder input, and should be read as scenario-based planning estimates rather than forecasts, because restoration duration depends on factors that are hard to specify in advance, including site access, inspection outcomes, and regional labor availability.

Operational strategies such as bus bridging and shared-ride services can reduce mobility impacts by adding temporary cross-hills capacity when rail service is constrained, but the achievable benefit varies by scenario and depends on operational constraints and cross-agency coordination. Stakeholder interviews with BART operations staff identified several limits on a bus bridge, including drivers' willingness to work overtime under emergency conditions, their ability to reach assignments after a major earthquake when their own homes and commute corridors may also be affected, and the capacity of partner agencies such as AC Transit and County Connection to redirect vehicles while meeting their own service obligations. These constraints evolve through the recovery period and are difficult to estimate in advance. The representative bus-bridging case in Section 6.4 quantifies one such strategy at the 654-year scenario under upper-bookend assumptions, and achievable mitigation in an actual event will fall below that bound.

Shared-ride options face a further barrier. Although transportation network companies have served as a surge-mobility and evacuation resource elsewhere (Wong et al., 2021a, 2021b; Brown, 2020), no established framework currently links BART to providers such as Uber and Lyft, so directing several hundred displaced passengers per peak hour to them is not operationally feasible under current arrangements. The model can test these strategies across scenarios, and identify which operational assumptions most influence the outcome, and can incorporate TNC-based options if that coordination develops.

Travel-demand management, including telework promotion, staggered work hours, and employer coordination, is a third operational measure that complements bus bridging and shared-ride partnerships. The model captures its effect through the recovery-stage demand level, where each reduction in peak demand represents travelers shifting away from cross-hills trips, so the demand sensitivity in Section 6.3.3 can be read in part as a sensitivity to travel-demand management uptake. This measure is especially attractive because the uncertainty quantification in Section 6.5.2 identifies recovery-stage demand as the dominant driver of travel-time variability, so measures that reduce peak demand act on the input that matters most. Travel-demand management also requires no new vehicles, drivers, or staging space and can be coordinated through public agencies and employers without depending on transit operators, though its effectiveness depends on the share of cross-hills trips with workplace flexibility and on employer participation.

7.2 Equity in Recovery-Stage Planning

Equity considerations should be integral to recovery-stage planning, particularly for cross-hills travelers in the Berkeley Hills corridor. A substantial share of transit riders are lower-income and depend on transit for access to employment, healthcare, and other essential services. BART's customer satisfaction surveys indicate that nearly 29 percent of riders are from households earning below $60,000 for a family of four (BART, 2022a), and the Los Angeles County Metropolitan Transportation Authority reports that approximately 83 percent of its riders have household incomes below $50,000 annually (LA Metro, 2022). Post-pandemic, BART's rider base remains more transit-dependent and lower-income than before the pandemic, as choice riders have not fully returned (BART, 2022a), and broader evidence shows that these populations are disproportionately lower-income and less likely to own a personal vehicle (Pucher & Renne, 2003; Sanchez et al., 2003). In the Berkeley Hills corridor, three constraints stack for transit-dependent BART riders during disruption. Many do not have access to a personal vehicle, no fixed bus route currently runs across the corridor, and ride-hail substitution carries a significantly higher per-trip cost than the BART fare it would replace (Soga et al., 2024).

These structural constraints translate into compounded burdens during disruption. Travelers with auto access can substitute when BART service is degraded; transit-dependent riders cannot. Travelers with discretionary trip purposes can defer or rearrange; those traveling for employment, healthcare, or other essential destinations face binding access constraints. Studies of post-disaster transportation recovery have repeatedly documented that carless and transit-dependent populations bear the most severe consequences when transit service is disrupted (Litman, 2006; Renne et al., 2008). In the modeling, travelers who remain on the degraded BART system absorb the added delay directly because they have no alternative, while the highest substitution costs fall on those who switch to ride-hail because they have no other choice. Both groups disproportionately include the populations least able to absorb either burden. Effective mitigation strategies should therefore be evaluated not only on aggregate travel-time impact but also on whether the time and cost burdens are distributed equitably across the affected population (Manaugh et al., 2015).

Recovery-stage planning should explicitly account for these distributional consequences. Pre-event investment in the substitute-route system should not assume that auto substitution is universally available; a complete strategy combines physical hardening of the alternates with operational mitigations such as a bus bridge that preserve a low-cost, transit-equivalent option for transit-dependent populations. Operational decisions should prioritize service quality on the corridors and trip purposes most relied upon by transit-dependent riders. Bus-bridge routing should match transit-dependent ridership patterns, fare policy during disruption should not impose access barriers on lower-income riders, and information dissemination should reach digitally underserved populations through accessible channels. The model can support these decisions by comparing mobility outcomes and substitution costs across recovery strategies, with explicit attention to the populations most affected. Stakeholder coordination on equitable substitute service is a productive direction for future applications of the model.

7.3 Seismic Damage Assessment of Transportation Infrastructure

A central aim of this work is to translate engineering-based infrastructure performance into mobility outcomes that practitioners can use and disseminate. High-fidelity seismic risk analysis is resource-intensive, so it is typically reserved for a single focal asset, and downstream transportation analyses therefore work with mixed-fidelity inputs, detailed for the focal asset and screening-level for the substitute facilities that absorb diverted demand. In this study, detailed seismic assessment was available for the Berkeley Hills Tunnel (Zengin et al., 2025), while the alternative cross-hills corridors were represented with standardized Hazus fragility and restoration relationships (FEMA, 2024). This mixed fidelity introduces uncertainty into the consequence estimates, and how best to combine high- and low-fidelity inputs is itself a methodological question.

Multi-fidelity uncertainty quantification methods, which combine sparse high-fidelity simulations with broader low-fidelity sampling, are well developed in the engineering literature (Peherstorfer et al., 2018) and have been applied to seismic risk at the structural level (Patsialis & Taflanidis, 2021). A common approach estimates the systematic gap between a high- and low-fidelity model of the same asset and uses it to correct low-fidelity predictions elsewhere (Kennedy & O'Hagan, 2000). Applying it here is limited by data, however, because anchoring the correction requires high-fidelity models of at least some substitute facilities, which are seldom available for ordinary cross-hills roads. The needed discrepancy therefore cannot be established within this study, and realizing this kind of correction will depend on future investment in higher-fidelity assessment of the substitute facilities, including the Caldecott Tunnel and the local-road alternatives.

As higher-resolution fragility, functionality, and recovery information becomes available for additional facilities, those inputs can replace the screening-level assumptions without changing the model architecture, allowing the analysis to be updated as data, methods, and post-event evidence improve.

7.4 Regional Impact Assessment and Travel Demand Uncertainty

Recovery-stage travel demand remains a dominant source of uncertainty for regional impact assessment, consistent with the variance-based decomposition in Section 6.5.2, which identifies it as the largest single driver of travel-time variability. Demand may fall through trip suppression, disrupted activity patterns, and changed work arrangements, while essential trips stay relatively high, particularly for travelers with limited flexibility in work location or travel options, and post-pandemic shifts in commute and mode preferences add further uncertainty. For these reasons, the demand assumptions used in this report should be interpreted as scenario definitions for comparative planning and stress testing, not as forecasts.

Rail disruption can also induce mode shifts that increase highway congestion and related externalities, as diversion from BART to private vehicles adds pressure to corridors already near capacity and can amplify travel-time impacts beyond the immediate disruption area (BART, 2022b). Extending the analysis to a Bay Area-wide assessment would build on the demand and capacity uncertainty treatments introduced here, adding clearly defined and internally consistent demand scenarios and improved empirical grounding for how trip making, route choice, and mode choice evolve across recovery stages.

8 References

American Association of State Highway and Transportation Officials (AASHTO). (2018). *A policy on geometric design of highways and streets* (7th ed.).

Anastasopoulos, I., Gerolymos, N., Drosos, V., Georgarakos, T., Kourkoulis, R., & Gazetas, G. (2008). Behaviour of deep immersed tunnel under combined normal fault rupture deformation and subsequent seismic shaking. *Bulletin of Earthquake Engineering*, *6*, 213–239.

Anderson, M. L. (2014). Subways, strikes, and slowdowns: The impacts of public transit on traffic congestion. *American Economic Review*, *104*(9), 2763–2796.

Asakura, T., & Sato, Y. (1998). Mountain tunnels damage in the 1995 Hyogoken Nanbu earthquake. *Quarterly Report of RTRI*, *39*, 9–16.

Basöz, N., Kiremidjian, A. S., Moore, J. E., Fan, Y., Yazlali, Ö., & Williams, M. (2007). Seismic risk assessment of transportation network systems. *Journal of Earthquake Engineering*, *11*(3), 371–382.

Bay Area Rapid Transit District (BART). (2022a). *Customer satisfaction survey 2022*.

Bay Area Rapid Transit District (BART). (2022b). *Local hazard mitigation plan*.

Bay Area Rapid Transit District (BART). (2025). *Ridership reports and dashboard*. https://www.bart.gov/about/reports/ridership

Ben-Akiva, M., & Lerman, S. R. (1985). *Discrete choice analysis: Theory and application to travel demand*. MIT Press.

Boeing, G. (2017). OSMnx: New methods for acquiring, constructing, analyzing, and visualizing complex street networks. *Computers, Environment and Urban Systems*, *65*, 126–139. https://doi.org/10.1016/j.compenvurbsys.2017.05.004

Brown, A. E. (2020). Who and where rideshares? Rideshare travel and use in Los Angeles. *Transportation Research Part A: Policy and Practice*, *136*, 120–134. https://doi.org/10.1016/j.tra.2020.04.001

California Department of Transportation (Caltrans). (2023). *2023 annual average daily traffic* [Data set]. https://dot.ca.gov/-/media/dot-media/programs/traffic-operations/documents/census/2023/2023-traffic-volumes-ca-a11y.xlsx

Chang, S. E. (2003). Transportation planning for disasters: An accessibility approach. *Environment and Planning A*, *35*(6), 1051–1072. https://doi.org/10.1068/a35195

Chang, S. E., & Nojima, N. (2001). Measuring post-disaster transportation system performance: The 1995 Kobe earthquake in comparative perspective. *Transportation Research Part A: Policy and Practice*, *35*(6), 475–494. https://doi.org/10.1016/S0965-8564(00)00003-3

Contra Costa Transportation Authority. (2018). *Caldecott Fourth Bore* [Fact sheet]. https://ccta.net/wp-content/uploads/2018/10/CCTA_Caldecott_Fourth_Bore_FS_v3.pdf

Federal Emergency Management Agency (FEMA). (2024). *Hazus earthquake model technical manual*. U.S. Department of Homeland Security. https://www.fema.gov/sites/default/files/documents/fema_hazus-earthquake-model-technical-manual-6-1.pdf

Giuliano, G., & Golob, J. (1998). Impacts of the Northridge earthquake on transit and highway use. *Journal of Transportation and Statistics, 1*(2), 1–20.

Hashash, Y. M. A., Hook, J. J., Schmidt, B., & Yao, J. I. C. (2001). Seismic design and analysis of underground structures. *Tunnelling and Underground Space Technology, 16*(4), 247–293. https://doi.org/10.1016/S0886-7798(01)00051-7

Iida, H., Hiroto, T., Yoshida, N., & Iwafuji, M. (1996). Damage to Daikai subway station. *Soils and Foundations*, *36*, 283–300.

Kennedy, M. C., & O'Hagan, A. (2000). Predicting the output from a complex computer code when fast approximations are available. *Biometrika*, *87*(1), 1–13. https://doi.org/10.1093/biomet/87.1.1

LA Metro. (2022). *Customer survey findings 2022*. Los Angeles County Metropolitan Transportation Authority.

Larcom, S., Rauch, F., & Willems, T. (2017). The benefits of forced experimentation: Striking evidence from the London Underground network. *Quarterly Journal of Economics*, *132*(4), 2019–2055.

LeBlanc, L. J., Morlok, E. K., & Pierskalla, W. P. (1975). An efficient approach to solving the road network equilibrium traffic assignment problem. *Transportation Research*, *9*(5), 309–318. https://doi.org/10.1016/0041-1647(75)90030-1

Litman, T. (2006). Lessons from Katrina and Rita: What major disasters can teach transportation planners. *Journal of Transportation Engineering*, *132*(1), 11–18.

Manaugh, K., Badami, M. G., & El-Geneidy, A. M. (2015). Integrating social equity into urban transportation planning: A critical evaluation of equity objectives and measures in transportation plans in North America. *Transport Policy*, *37*, 167–176.

McCullough, H. (1994). *Earthquake damage to transportation systems* [Report]. U.S. Department of Commerce, National Oceanic and Atmospheric Administration, National Weather Service.

McFadden, D. (1974). Conditional logit analysis of qualitative choice behavior. In P. Zarembka (Ed.), *Frontiers in econometrics* (pp. 105–142). Academic Press.

McKenna, F., Gavrilovic, S., Zsarnóczay, A., Zhong, K., & Elhaddad, W. (2025). *NHERI SimCenter R2DTool* (Version 1.2.0) [Computer software]. Zenodo. https://doi.org/10.5281/zenodo.14800304

Metropolitan Transportation Commission. (2011). *Caldecott Fourth Bore Project* [Fact sheet]. https://mtc.ca.gov/sites/default/files/Caldecott_Fourth_Bore_Fact_Sheet.pdf

Owen, G. N., & Scholl, R. E. (1981). *Earthquake engineering of large underground structures* (Report No. FHWA IRD 80 1195). Federal Highway Administration.

Patsialis, D., & Taflanidis, A. A. (2021). Multi-fidelity Monte Carlo for seismic risk assessment applications. *Structural Safety, 93*, 102129. https://doi.org/10.1016/j.strusafe.2021.102129

Peherstorfer, B., Willcox, K., & Gunzburger, M. (2018). Survey of multifidelity methods in uncertainty propagation, inference, and optimization. *SIAM Review*, *60*(3), 550–591. https://doi.org/10.1137/16M1082469

Pel, A. J., Bliemer, M. C. J., & Hoogendoorn, S. P. (2012). A review on travel behaviour modelling in dynamic traffic simulation models for evacuations. *Transportation*, *39*(1), 97–123.

Pucher, J., & Renne, J. L. (2003). Socioeconomics of urban travel: Evidence from the 2001 NHTS. *Transportation Quarterly*, *57*(3), 49–77.

Renne, J. L., Sanchez, T. W., & Litman, T. (2008). *National study on carless and special needs evacuation planning: A literature review*. University of New Orleans Transportation Center.

Russo, M., Germani, G., & Amberg, W. (2002). Design and construction of large tunnel through active faults: A recent application. In *Proceedings of the International Conference of Tunneling and Underground Space Use* (pp. 1–14). Istanbul, Turkey.

Sanchez, T. W., Stolz, R., & Ma, J. S. (2003). *Moving to equity: Addressing inequitable effects of transportation policies on minorities*. Civil Rights Project, Harvard University.

Sheffi, Y. (1985). *Urban transportation networks: Equilibrium analysis with mathematical programming methods*. Prentice Hall.

Soga, K., Comfort, L., Zhao, B., Tang, Y., & Han, T. (2024). *Assessing the functionality of transit and shared mobility systems after earthquakes* (Report No. UC ITS RIMI 4K). Institute of Transportation Studies, University of California, Berkeley. https://doi.org/10.7922/G2NZ860C

Train, K. E. (2009). *Discrete choice methods with simulation* (2nd ed.). Cambridge University Press.

Transportation Research Board (TRB). (2022). *Highway capacity manual* (7th ed.). National Academies of Sciences, Engineering, and Medicine.

Uenishi, K., & Sakurai, S. (2000). Characteristic of the vertical seismic waves associated with the 1995 Hyogo-ken Nanbu (Kobe), Japan earthquake estimated from the failure of the Daikai Underground Station. *Earthquake Engineering and Structural Dynamics*, *29*(6), 813–821.

Ulusay, R., Aydan, Ö., & Hamada, M. (2002). The behaviour of structures built on active fault zones: Examples from the recent earthquakes of Turkey. *Structural Engineering/Earthquake Engineering*, *19*(2), 149–167.

United States Geological Survey (USGS). (2016). *Earthquake outlook for the San Francisco Bay region 2014–2043* (Fact Sheet 2016–3020). https://pubs.usgs.gov/fs/2016/3020/fs20163020.pdf

Wang, C., Wang, D., & Chen, Q. (2021). Regional evaluation of liquefaction-induced lateral ground deformation for city-scale transportation resilience analysis. *Journal of Infrastructure Systems*, *27*(2), 04021008. https://doi.org/10.1061/(ASCE)IS.1943-555X.0000601

Wang, W. L., Wang, T. T., Su, J. J., Lin, C. H., Seng, C. R., & Huang, T. H. (2001). Assessment of damage in mountain tunnels due to the Taiwan Chi-Chi earthquake. *Tunnelling and Underground Space Technology*, *16*(3), 133–150.

Wardrop, J. G. (1952). Some theoretical aspects of road traffic research. *Proceedings of the Institution of Civil Engineers, Part II*, *1*(3), 325–378. https://doi.org/10.1680/ipeds.1952.11362

Werner, S. D., Taylor, C. E., Moore, J. E., II, Walton, J. S., & Cho, S. (2006). *REDARS 2: Methodology and software for seismic risk analysis of highway systems* (MCEER-06-SP08). Multidisciplinary Center for Earthquake Engineering Research, University at Buffalo.

Wong, S. D., Walker, J. L., & Shaheen, S. A. (2021a). Bridging the gap between evacuations and the sharing economy. *Transportation*, *48*(3), 1409–1458. https://doi.org/10.1007/s11116-020-10101-3

Wong, S. D., Walker, J. L., & Shaheen, S. A. (2021b). Trust and compassion in willingness to share mobility and sheltering resources in evacuations: A case study of the 2017 and 2018 California wildfires. *International Journal of Disaster Risk Reduction*, *52*, 101900. https://doi.org/10.1016/j.ijdrr.2020.101900

Yu, H., Chen, J., Yuan, Y., & Zhao, X. (2016). Seismic damage of mountain tunnels during the 5.12 Wenchuan earthquake. *Journal of Mountain Science*, *13*, 1958–1972.

Zengin, E., Bozorgnia, Y., & Stewart, J. P. (2025). *Evaluating the seismic vulnerability and resilience of BART's Berkeley Hills Tunnel*. Institute of Transportation Studies, University of California. https://doi.org/10.7922/G22J697K

Zhao, T. T., & Zhang, Y. (2020). Transportation infrastructure restoration optimization considering mobility and accessibility in resilience measures. *Transportation Research Part C: Emerging Technologies*, *117*, 102700. https://doi.org/10.1016/j.trc.2020.102700